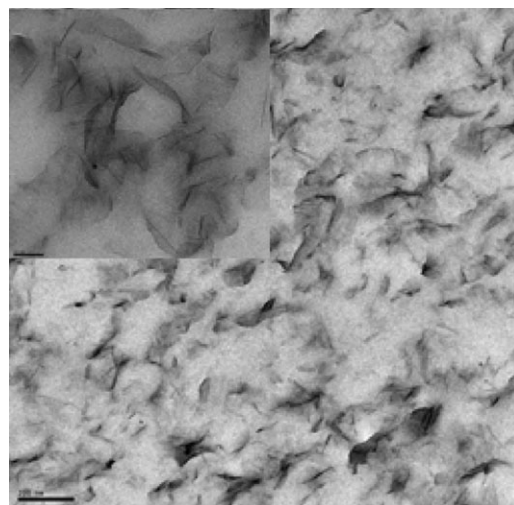


# Correlation between Composition, Structure and Properties of Poly(lactic acid)/Polyadipate-Based Nano-Biocomposites

Verónica P. Martino, Roxana A. Ruseckaite, Alfonso Jiménez,\* Luc Averous

Poly(lactic acid) plasticized with 15 and 20 wt.-% of polyadipate was melt-blended with different amounts of an O-MMT (1–5 wt.-%) to prepare nano-biocomposites. The effect of plasticizer and nanofiller contents on the morphology and on thermal, mechanical and barrier properties of PLA-based nano-biocomposites was evaluated in order to understand their structure-properties relationships. The oxygen transmission rate was notably reduced (around 45%) with increasing amount of clay due to an increased tortuosity. However, for clay concentrations above 3 wt.-%, a significant detriment in ductile properties could also be observed. For a given amount of nanofiller, the increasing plasticizer concentration improved the clay dispersion through the polymeric matrix.



## Introduction

The use of plasticized poly(lactic acid) (PLA) has shown promising results to obtain flexible films. The presence of a plasticizer decreases the glass transition temperature of PLA, reduces the aging effects typically found in neat PLA, improves its ductility and consequently broadens the range of potential applications.<sup>[1,2]</sup> Among all the plasticizers tested for the preparation of such materials,<sup>[3–5]</sup> polyadi-

pates have shown good performance.<sup>[6,7]</sup> They combine a relatively good compatibility with PLA with their high molar mass to limit their migration towards the polymer surface. However, some of their properties do not fulfill the requirements for some applications, in particular their barrier properties which decrease significantly after plasticization. The addition of nanofillers has demonstrated a great potential to improve such properties as it has already been reported.<sup>[8–11]</sup>

Nano-biocomposites formed by a biopolymer and layered silicates as reinforcement agents often show improved barrier and mechanical properties, oxidation stability and eventually, tunable biodegradability.<sup>[12–14]</sup> Layered silicates, in particular montmorillonite (MMT), are naturally occurring and low-cost materials. The use of hydrophobic polymeric matrices, such as PLA, makes necessary their blending with organomodified layered montmorillonite (O-MMT).<sup>[12–16]</sup> The addition of O-MMT

V. P. Martino, A. Jiménez

Department of Analytical Chemistry, Nutrition & Food Sciences,  
University of Alicante, Crta. Alicante – San Vicente s/n, 03690 San  
Vicente del Raspeig, Spain

E-mail: alfjimenez@ua.es

V. P. Martino, L. Averous

LIPHT-ECPM, EAC(CNRS) 4379, Université de Strasbourg, 25 rue  
Bequerel, 67087 Strasbourg Cedex 2, France

R. A. Ruseckaite

Research Institute of Material Science and Technology (INTEMA),  
CONICET-Engineering Faculty, Juan B. Justo 4302, Mar del Plata.  
Buenos Aires, Argentina

has been investigated as a mean to increase crystallinity and to improve the thermal and mechanical properties of PLA.<sup>[17]</sup> The modification of MMT leads to better compatibility with PLA, since the surfactants are able to reduce the interface energy and to improve wetting with the polymer.<sup>[18]</sup> However, the degree of intercalation-exfoliation strongly depends not only on the matrix and filler nature but also on the processing method.<sup>[19]</sup> Pluta et al.<sup>[20]</sup> studied the effect of the O-MMT content (1–10 wt.-%) with different modifications as reinforcing agent of PLA plasticized with 20 wt.-% poly(ethylene glycol) (PEG) as matrix. Both, PLA and PEG chains, seemed to intercalate into clay platelets at certain degree, and authors reported that exfoliation could be achieved depending on the organic modification of MMT. Concerning dynamic mechanical properties of these nano-biocomposites, some mechanical losses were observed with the increasing amount of nanofiller and they were correlated with the intercalation magnitude and the ability of PEG molecules to penetrate the silicate galleries. Other authors reported an important improvement in oxygen barrier properties (up to 48%) by the addition of 5 wt.-% O-MMT to PLA plasticized with a citrate ester without any strong decrease in ductile properties.<sup>[21]</sup>

In a previous work<sup>[22]</sup> we reported that polyadipates were able to swell the clay prior to melt blending, increasing the gallery space and facilitating the migration of PLA chains between platelets. Both, an improvement in the nanofiller dispersion and some increase in the number of exfoliated structures without any significant thermomechanical degradation were observed. The addition of a low amount of filler (2.1 wt.-%) conducted to an important increase in the oxygen barrier property (around 25%) without detrimental effects in ductility. However, properties of PLA-based nano-biocomposites showed some strong evolution by aging.<sup>[23,24]</sup> Pluta et al. studied physical properties of plasticized PLA nanocomposites.<sup>[25]</sup> They reported that samples were not stable over time since all of them suffered undesirable changes with phase separation and plasticizer migration to the sample surface. These changes were higher for unfilled plasticized PLA than for the corresponding nano-biocomposites, since the presence of clay platelets reduced the physical aging rate.

The main goal of this work is to analyze the structure/properties relationships of nano-biocomposites based on plasticized PLA with O-MMT, prepared by melt intercalation. Since final properties are strongly dependent on the structure, this paper is first dedicated to the determination of clay organization in the matrix. The effects of plasticizer and nanofiller contents on the thermal, mechanical and oxygen barrier properties were also studied. In addition, aging studies were carried out under controlled storage conditions. Overall migration tests were also performed according to EU regulations<sup>[26]</sup> as a first approach to

evaluate potential applications of plasticized PLA and nano-biocomposites as food contact materials.

## Experimental Part

### Material and Sample Preparation

Poly(lactic acid) (CML PLA,  $\overline{M}_n = 63\,000 \pm 12\,000$  Da,  $T_g = 58^\circ\text{C}$ ) was purchased from Tate & Lyle (Turku, Finland). A commercial polyadipate identified with the trade name Glyplast<sup>®</sup> 206/7 (G206/7,  $\overline{M}_n = 2\,565$  Da;  $T_g = -54^\circ\text{C}$ ) was kindly supplied by Condensia Química S.A (Barcelona, Spain) and was described elsewhere.<sup>[6]</sup> Commercial O-MMT Cloisite<sup>®</sup>-30B (C30B, CEC = 90 mequiv. per 100 g clay) was provided by Southern Clay Products Inc (TX, USA). This O-MMT is based on a quaternary ammonium surfactant,  $N^+(\text{Me})(\text{EtOH})_2(\text{tallow})$ , with 30 wt.-% organics content.

PLA and clay were dried under vacuum overnight at  $80^\circ\text{C}$  while plasticizers were dried at  $55^\circ\text{C}$  during 2 h in desiccator with  $\text{P}_2\text{O}_5$ . They were further kept for more than 24 h in desiccator under vacuum until using.

Nano-biocomposites were prepared according to the following processing conditions. Different amounts of filler (1, 3 and 5 wt.-% related to the plasticized PLA matrix) were first swelled at two different plasticizer concentrations (15 and 20 wt.-% on PLA basis) and sonicated during 2 h at  $60^\circ\text{C}$ . After manual homogenization with PLA at ambient temperature, materials were added into a Haake Rheomix 600 internal mixer (Karlsruhe, Germany) and melt-blended at 100 rpm during 20 min. The processing temperature was set at  $170^\circ\text{C}$  but it increased to  $190^\circ\text{C}$  upon mixing. Blends were then processed into films (170–200  $\mu\text{m}$  thick) and sheets (0.8–0.9 mm thick) by compression molding at  $180^\circ\text{C}$  in a hot press (Collin GmbH, Ebersberg, Germany) using stainless steel frames (16  $\times$  16  $\text{cm}^2$ ) to ensure constant thickness. Materials were kept between the hot plates at atmospheric pressure for 5 min until melting and then they were pressed in a multistep process (under 5 MPa for 1 min, 10 MPa for 1 min and 20 MPa for 6 min) to remove air bubbles. Samples were then cooled to room temperature with circulating water under pressure (20 MPa). Visual aspect of nano-biocomposite films changed in color from completely colorless and transparent for the neat matrix to yellowish and brownish when adding 3 and 5 wt.-% C30B, respectively. The corresponding unfilled plasticized PLA samples were prepared by using the same processing conditions and they were used as controls.

### Methods and Techniques

DSC tests were conducted on a TA Instruments DSC Q-2000 (New Castle, DE, USA) under nitrogen atmosphere (50  $\text{mL} \cdot \text{min}^{-1}$ ). The main thermal parameters were determined in a second scan at  $10^\circ\text{C} \cdot \text{min}^{-1}$  from  $-90$  to  $+180^\circ\text{C}$ . Thermal history of samples (5–10 mg placed in an aluminum pan) was erased during the first scan at  $10^\circ\text{C} \cdot \text{min}^{-1}$  from room temperature up to  $180^\circ\text{C}$ , followed by 5 min at this temperature and quenching to  $-90^\circ\text{C}$ .

Thermogravimetric analysis (TGA) was performed in a TGA/SDTA 851 Mettler Toledo thermal analyzer (Schwarzenbach, Switzerland). Samples were heated from room temperature up to  $600^\circ\text{C}$  at  $10^\circ\text{C} \cdot \text{min}^{-1}$  under oxygen atmosphere (50  $\text{mL} \cdot \text{min}^{-1}$ ).

Wide angle X-ray scattering (WAXS) patterns of films were recorded with a Seifert diffractometer, model JSO-DebyeFlex 2002 equipped with Cu K $\alpha$  radiation source ( $\lambda = 0.1546$  nm), operating at 40 kV and 40 mA as the applied voltage and current, respectively. The incidence angle was varied between 2 and 90° at a scanning rate of 1° · min<sup>-1</sup>. Small angle X-ray scattering (SAXS) was performed to determine the intercalation/exfoliation degree of nanocomposites, using a powder diffractometer Siemens D-5000 (Munich, Germany) using Cu K $\alpha$  radiation source ( $\lambda = 0.1546$  nm). The incidence angle was varied from 2 to 10° with step size 0.015° and step time 4 s (scanning rate 0.225° · min<sup>-1</sup>).

Transmission electron microscopy (TEM) images were recorded with a JEOL JEM-2010 (Tokyo, Japan) microscope using an accelerating voltage of 100 kV. Samples were previously ultramicrotomed (RMC, model MTXL) in order to obtain slices 100 nm thick.

Tensile tests were carried out with a uniaxial tensile testing machine IBERTEST ELIB 30 (Ibertest, Madrid, Spain) according to the standard procedure (ASTM D882-01)<sup>[27]</sup> at a crosshead speed of 10 mm · min<sup>-1</sup> and ambient temperature (23 °C). Average percentage deformation at break ( $\epsilon\%$ ) and elastic modulus (E) were calculated from the resulting stress/strain curves as the average of five measurements.

The oxygen transmission rate (OTR) was measured in 14 cm diameter circle films with an oxygen permeation analyzer from Systech Instruments, model 8500 (Metrotec S.A, Spain). Various samples were prepared for each formulation. Equilibrated films were clamped in a diffusion chamber where pure oxygen (99.9% purity) was introduced into the upper half, while nitrogen was injected into the lower half of the chamber where an oxygen sensor was placed.

Selected formulations were submitted to aging studies after 2 months of storage at 25 °C and 50% relative humidity (RH) in a Dycometal-CM81 climatic testing chamber (Barcelona, Spain).

Overall migration tests were performed under the general conditions established in UNE-EN 1186 standard,<sup>[26]</sup> (10 d, 40 °C). Tests were performed using a surface area of 10 cm<sup>2</sup> by total immersion in 100 mL of olive oil as fatty simulant (UNE-EN 1186-2)<sup>[28]</sup> and distilled water as aqueous simulant (UNE-EN 1186-3).<sup>[29]</sup>

## Results and Discussion

### Nano-Biocomposites Structure

The swelling process of the clay by the plasticizer was investigated by analyzing the SAXS patterns of various C30B/polyadipate mixtures assisted by sonication. Figure 1 shows the SAXS patterns of mixtures prepared between G206/7 and different amounts of C30B (1, 3 and 5 wt.-% related to the PLA matrix plasticized with 15 wt.-% of G206/7), before melt-blending. The interlayer distances (calculated from Bragg's law) decreased with the increasing amount of clay, since results were 43, 41 and 38 Å for 1, 3 and 5 wt.-% C30B, respectively. The basal d-spacing ( $d_{001}$ ) for the pristine clay was 18 Å.<sup>[22]</sup>

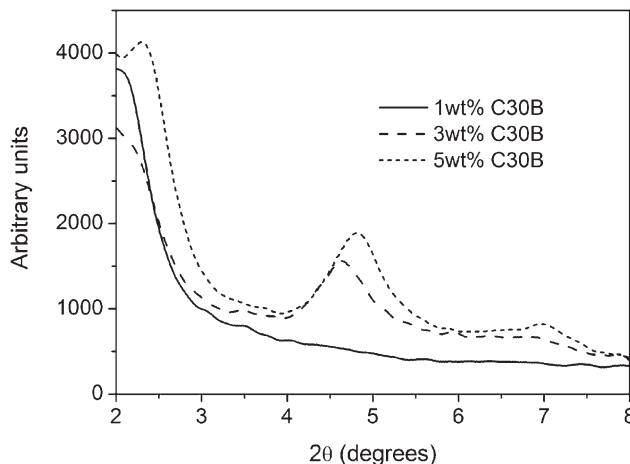


Figure 1. SAXS patterns of clay/plasticizer mixtures after sonication at 60 °C during 2 h for 15 wt.-% G206/7 and different amounts of C30B.

The effect of the plasticizer content on the final structure of nano-biocomposites prepared with a fixed amount of clay can be observed in the SAXS patterns shown in Figure 2, since the intensity of curves diminished with increasing amounts of plasticizer. This could be linked to a better dispersion of the nanofiller through the matrix favored by the polyadipate. However, this effect was only noticeable at the highest clay content where volume restriction could occur. At lower contents neither peaks nor even shoulders were observed by SAXS (data not shown).

Figure 3 shows representative TEM micrographs of various nano-biocomposites. It could be concluded that the best dispersion was obtained for low clay contents (Figure 3a–c). Whatever the polyadipate concentration, there were no significant differences for nano-biocomposites based on 1 wt.-% C30B since any apparent tactoids

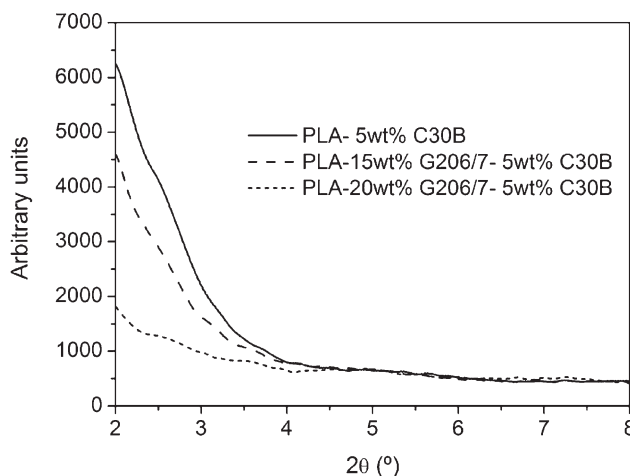
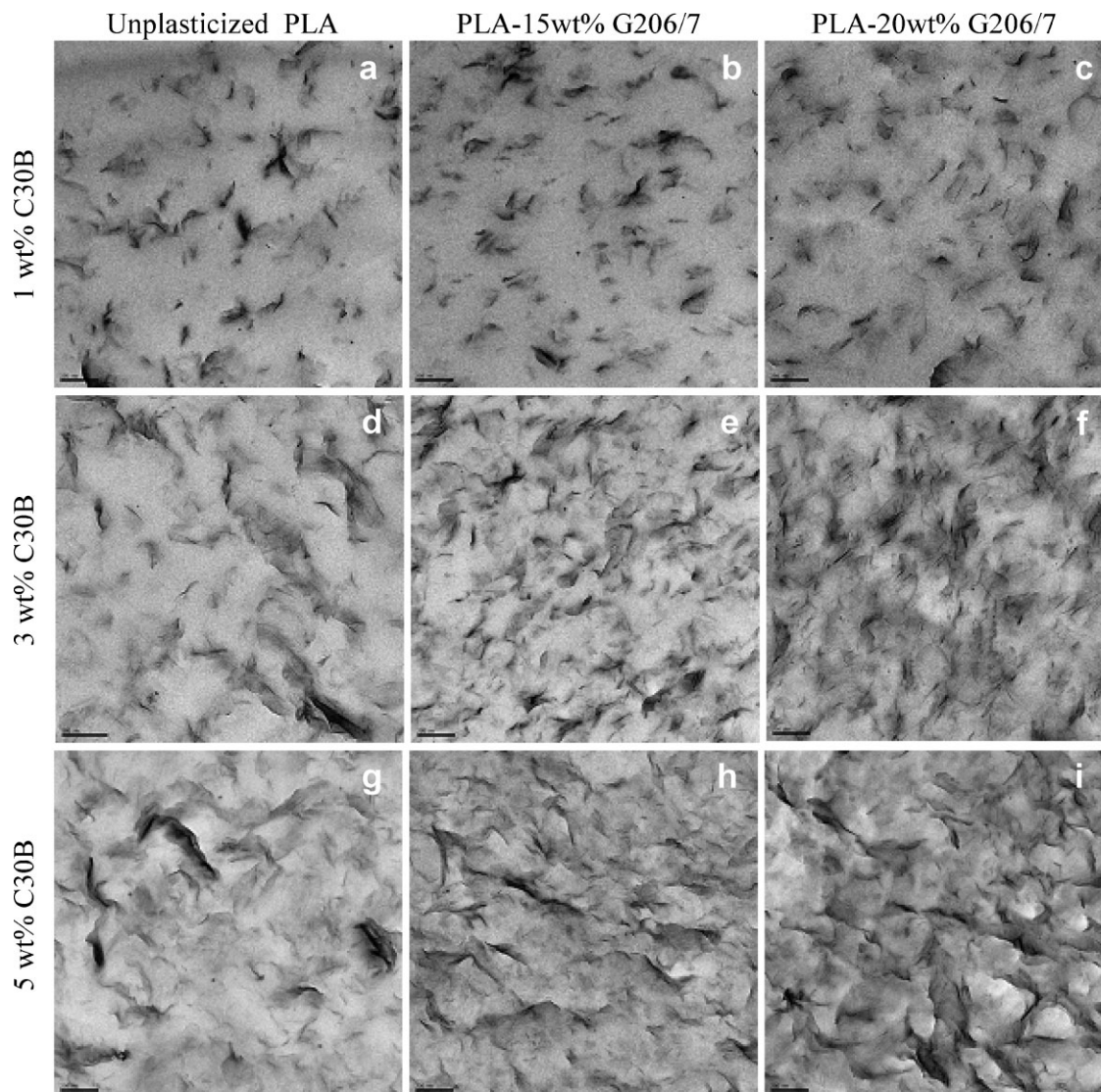


Figure 2. SAXS patterns of nano-biocomposites with 5 wt.-% C30B and different plasticizer contents.



**Figure 3.** TEM micrographs of nano-biocomposites with C30B at 1 wt.-% (a–c); 3 wt.-% (d–f) and 5 wt.-% (g–i) for the different matrices (reference bar: 200 nm).

and/or agglomerates were observed in plasticized PLA nano-biocomposites. Nevertheless, by increasing the nano-filler amount, the plasticizer favors the clay dispersion conducting to more homogeneous structures. For instance, the clay distribution seemed lower for un-plasticized nano-biocomposites with 3 wt.-% C30B (Figure 3d) compared to plasticized materials (Figure 3e,f). This effect could also be clearly observed at the highest clay amount (5 wt.-%), since only few individual platelets were observed for un-plasticized nano-biocomposites where some tactoids and even agglomerates appeared, with maximum dimensions around  $250\text{ nm} \times 1.8\text{ }\mu\text{m}$  (Figure 3g). Although some agglomerates were also observed in the case of plasticized systems (Figure 3h,i), they were present at lower amounts and with smaller dimensions. Besides, such randomly

distributed agglomerates were not noticeable with identified peaks by SAXS, as observed in Figure 2.

As it was already shown in a previous work,<sup>[22]</sup> the addition of C30B (2.1 wt.-%), favored the crystallization of PLA chains. DSC thermograms of samples with clay content varying from 1 to 5 wt.-% exhibited similar behavior to that already reported. The crystallization peak of nano-biocomposites shifted to lower temperatures when compared to the corresponding unfilled matrices. This effect was more noticeable with 20 wt.-% of plasticizer (Figure 4). The nanosized layered platelets with large surface area, especially for the C30B composite having an exfoliated structure, enhance this crystallization ability.<sup>[16]</sup> Nano-biocomposites showed two melting peaks indicating the presence of crystals with different degree of perfection.

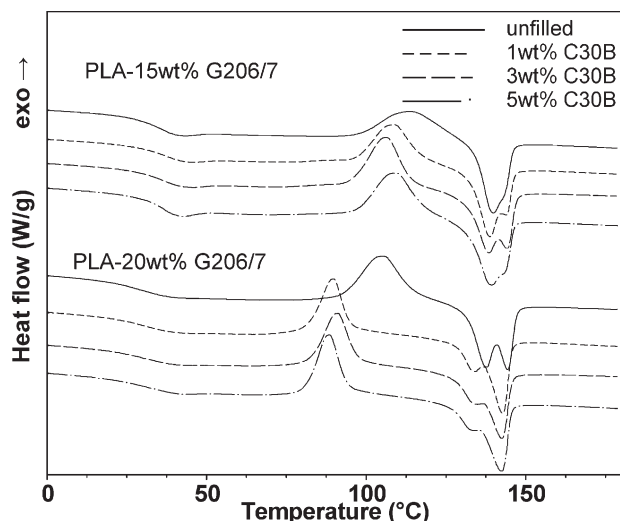


Figure 4. DSC curves obtained during the first heating of plasticized PLA and nano-biocomposites with different amounts of clay.

Table 1 shows  $T_g$  values obtained during the second heating step of samples by DSC. No significant differences with increasing amounts of clay were observed, as all values were close to those obtained for the corresponding unfilled matrices. This result is interesting as it suggests that there is no competition between the plasticizer and PLA chains for interacting with the nanofiller. Consequently the polyadipate could keep its plasticizing effect even after the elaboration of the nano-biocomposites. Therefore, it could be concluded that interactions between PLA and polyadipate are stronger than those between polyadipate and clay.

Table 1. Glass transition temperature ( $T_g$ ), and thermal degradation parameters of plasticized PLA and nano-biocomposites with 1, 3 and 5 wt.-% C30B determined under oxygen atmosphere.

G206/7	C30B	$T_g$	IDT <sup>b)</sup>	$T_{max}$
wt.-%	wt.-%	°C <sup>a)</sup>	°C	°C <sup>c)</sup>
15	0	37.6	316	364
	1	37.4	317	362
	3	37.7	326	365
	5	36.1	326	366
20	0	31.1	314	365
	1	32.8	313	362
	3	30.5	324	364
	5	31.6	324	365

<sup>a)</sup>Determined by DSC at  $10\text{ °C} \cdot \text{min}^{-1}$  during the second heating step; <sup>b)</sup>Determined by TGA at  $\alpha = 0.05$  ( $10\text{ °C} \cdot \text{min}^{-1}$ ); <sup>c)</sup>Determined from the maximum of DTG curves.

## Thermal Characterization

Table 1 also summarizes the main thermal parameters obtained by TGA for all nanocomposites, including initial decomposition temperature (IDT) and temperature at the maximum degradation rate ( $T_{max}$ ). The addition of 1 wt.-% clay did not change the thermal stability of nanocomposites since no important variations in IDT and  $T_{max}$  were observed compared to the unfilled counterparts. However, further clay additions led to an increment in IDT around  $10\text{ °C}$  for 3 wt.-% C30B (Table 1) suggesting a delay in the beginning of the thermal decomposition process. Increasing the clay content to 5 wt.-% did not induce any other improvement in thermal stability. On the other hand, whatever the clay content, the maximum degradation rate for nanocomposites as well as unfilled matrices was centered at temperatures between  $362$  and  $366\text{ °C}$  (Table 1). These results are in good agreement with our previous work based on 2.1 wt.-% C30B and 15 wt.-% G206/7 where the increment in IDT was about  $7\text{ °C}$  without significant  $T_{max}$  shifts.<sup>[22]</sup> Clay and char formed during thermal oxidation might act as heat barrier,<sup>[16]</sup> but only at the first stages of this process while they could keep heat and then accelerate the degradation at higher temperatures.

## Barrier Properties

The effect of clay content on the OTR for plasticized PLA nano-biocomposites at different polyadipate concentrations is summarized in Table 2. It could be observed that the oxygen permeation through the plasticized films was considerably reduced with increasing amounts of clay. Whatever the plasticizer concentration, nano-biocomposites suffered a reduction in OTR. Such decrease was 15, 36 and 44% for 1, 3 and 5 wt.-% C30B, respectively, compared to the unfilled counterparts. A similar behavior was observed for the unplasticized system, where OTR.e values decreased

Table 2. OTR per film thickness (OTR.e) of plasticized PLA films and nano-biocomposites with 1, 3 and 5 wt.-% C30B (all indicated percentages are in wt.-%).

Sample	OTR.e
	$\text{cm}^3 \cdot \text{mm} \cdot \text{m}^{-2} \cdot \text{d}^{-1}$
PLA-15% G206/7	$30.9 \pm 0.6$
PLA-15% G206/7-1% C30B	$26.2 \pm 0.6$
PLA-15% G206/7-3% C30B	$19.7 \pm 2.2$
PLA-15% G206/7-5% C30B	$16.7 \pm 2.9$
PLA-20% G206/7	$37.7 \pm 4.0$
PLA-20% G206/7-1% C30B	$32.5 \pm 2.4$
PLA-20% G206/7-3% C30B	$23.8 \pm 0.3$
PLA-20% G206/7-5% C30B	$21.4 \pm 2.2$

approximately in the same proportion with the increasing amount of C30B. These results were similar to those obtained by other authors for PLA-based nano-biocomposites.<sup>[10,21]</sup> It is known that the improvement in barrier properties for nanocomposites can be caused by two effects, the increase in path tortuosity for the gas molecules to move through the material structure and the eventual evolution of the material crystallinity.<sup>[10]</sup> This last point was checked and some additional structural tests were performed. DSC thermograms showed that all materials were amorphous after processing, since crystallization and melting peak areas were similar (Figure 4). WAXS patterns confirmed the amorphous structure of all matrices since no diffraction peaks at angles around 18° due to PLA crystals were observed. Therefore it could be concluded that the improved barrier property of PLA nanocomposites was mainly due to the clay dispersion all through the matrix.

### Tensile Properties

Figure 5 shows the results for tensile tests of plasticized PLA matrices as well as for their nano-biocomposites. As it could

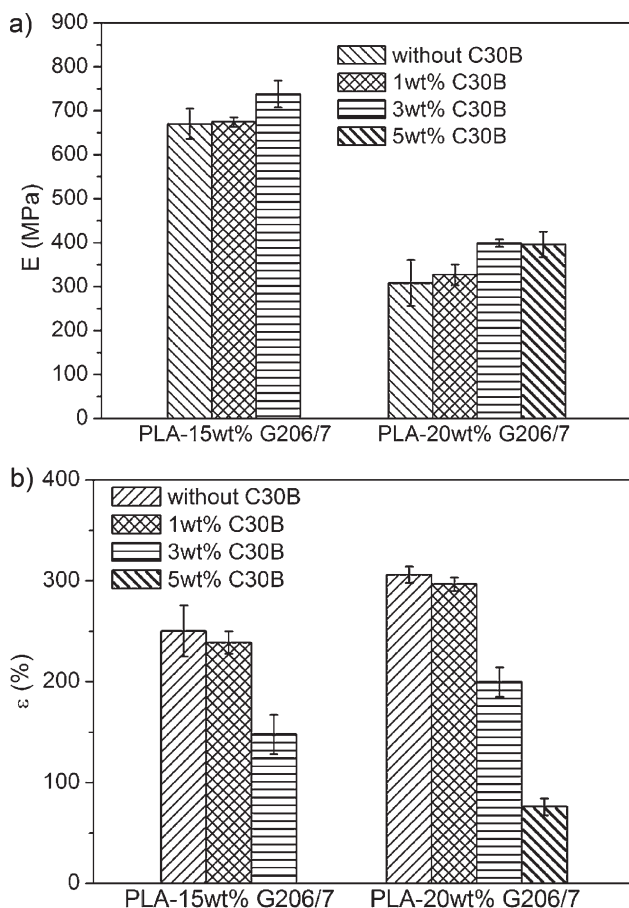


Figure 5. (a) Elastic modulus  $E$  and (b) percentage deformation at break  $\epsilon_B$  for plasticized PLA and nano-biocomposites for different nanofiller amounts.

be expected, the addition of clay increased the elastic modulus ( $E$ ) and reduced the elongation at break ( $\epsilon_B$ ) when amounts of C30B higher than 1 wt.-% were added. For both plasticizer concentrations and compared to the unfilled matrices, at 1 wt.-% clay content no significant changes in tensile properties were observed (Figure 5). However at 3 wt.-% clay, increments in  $E$  values were about 10 and 30%, while reductions in  $\epsilon_B$  were 40 and 35%, for plasticizer concentrations 15 and 20 wt.-%, respectively. By increasing the amount of clay up to 5 wt.-% the material became so brittle that cutting the specimens in the case of formulation with the lowest plasticizer content (15 wt.-%) without introducing cracks, was almost impossible and tests could not be performed. Materials with 20 wt.-% plasticizer and 5 wt.-% of clay exhibited similar  $E$  values to those with 3 wt.-% of C30B, but the deformation at break suffered a reduction of about 75% compared to the unfilled plasticized counterpart. Anyway, these results showed that some plasticization could still be observed at high clay amounts, since the elastic modulus was lower than results for neat PLA (around 2 GPa) and elongation at break was clearly higher (around 6% for the neat polymer).<sup>[7]</sup>

These results are in good agreement with TEM observations, where formulations with 5 wt.-% clay showed tactoids and even some agglomerates increasing the material brittleness. At 3 wt.-% clay, although only few small tactoids were observed, nano-biocomposites could decrease the break values. Therefore, two different effects on the elongation of these materials could be combined. These effects could be linked to (i) the presence of tactoids and agglomerates and (ii) the addition of inorganic filler to a polymeric matrix. Both effects influence the values at break and increase with the nanofiller content leading to new evidence of the better clay dispersion obtained at higher plasticizer concentration.

### Aging Studies

From the above-referred results it was concluded that the best properties were obtained for nano-biocomposites with 3 wt.-% C30B at both polyadipate concentrations (15 and 20 wt.-%). Therefore, these formulations as well as the corresponding unfilled matrices were chosen for further characterization after 2 months of storage under controlled conditions (25 °C and 50% RH).

It was observed that the clay addition reduced the aging of samples since the shift to lower crystallization temperatures observed by DSC was higher for the unfilled matrices, compared to the corresponding unaged material (Figure 6). This effect was more clearly evidenced for formulations with 20 wt.-% polyadipate in which the crystallization temperature shift was around 24 °C, while for the corresponding nano-biocomposite it was around 15 °C. This result could be explained if considering that the presence of clay could restrict the segmental motions at the

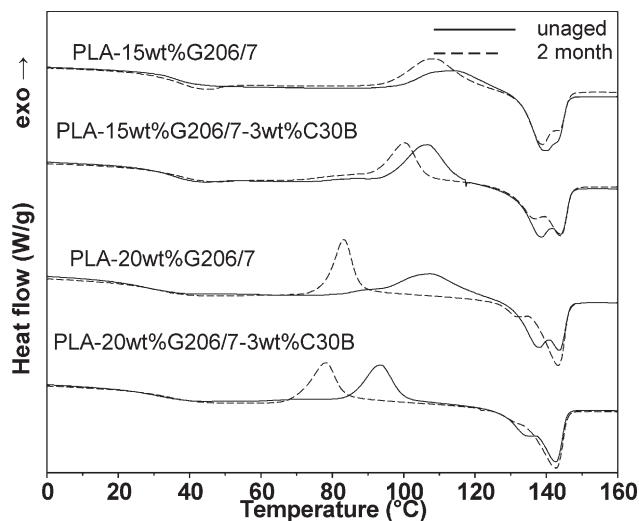


Figure 6. DSC curves obtained during the first heating step for plasticized PLA samples and the corresponding nano-biocomposites with 3 wt.-% C30B before and after 2 months of storage.

organic-inorganic interface when the storage temperature is below  $T_g$ , as in this case. Therefore, chain reaccommodations and matrix densification would be less important for nano-biocomposites than for the unfilled counterparts. Similar results were reported by Pluta et al.<sup>[25]</sup> who studied physical aging of PLA plasticized with PEG and nano-biocomposites with C30B. Authors stated that the extent of properties changed and phase separation was much higher for unfilled plasticized PLA than for nano-biocomposites since clay reduced the physical aging rate.

It was expectable that such structural rearrangements caused by aging process could show some impact on the materials barrier and mechanical properties. A reduction in OTR.e values was observed due to the decrease in free volume for gas diffusion through the matrix (Table 3). In agreement with DSC observations, such increase in the oxygen barrier property compared to unaged samples (Table 2) was lower for the nano-biocomposites (around 13% vs. 19–20% for the unfilled plasticized PLA). Regarding mechanical properties, a slight increment in the elastic

modulus and a reduction in the elongation at break were observed, in particular for the formulations with higher plasticizer amount (Table 3). This was linked to certain matrix densification due to the aging process, although samples remained amorphous as it was verified by WAXS patterns. However, taking into account the standard deviations, such evolutions were not important (Figure 5 and Table 3, before and after 2 months storage, respectively).

### Overall Migration

Table 3 also shows the overall migration values obtained for the two food simulants used in this work (distilled water and olive oil). The diffusion process could be caused by the mass transfer of chemical components involved in these materials, i.e., polyadipate, residual lactic acid, oligomeric lactic acid (eventually present due to chain scission during processing), and the clay itself. However, due to its higher concentration in the matrix and the relative low average molar mass, the plasticizer was expected to migrate in a higher amount, in particular in the fatty simulant due to its non-polar nature (Table 3).

The overall migration limit established by the current European legislation concerning food contact materials is  $10 \text{ mg} \cdot \text{dm}^{-2}$ .<sup>[30]</sup> In water simulant none of the studied materials exceeded such limit. In opposition, the only formulation that fulfilled this requirement in oil simulant was PLA-15 wt.-% G206/7 and the corresponding nano-biocomposite. It must be taken into account that the testing temperature selected for this study (and indicated by legislation) was  $40^\circ\text{C}$ , higher than the  $T_g$  values of the matrices (Table 1). Therefore, it was likely that samples suffered some annealing during the testing period (10 d) and developed some crystallinity facilitating the plasticizer exudation. Such effects were more pronounced at high plasticizer amount and/or the presence of clay acting as nuclei for the crystallization process. Nevertheless, it is advisable that performing these tests at lower temperatures (e.g.,  $20^\circ\text{C}$ , as indicated in the referred Commission Directive for packaging materials in contact with refrigerated food<sup>[30]</sup>) should lead to acceptable overall migration levels in fatty simulants.

Table 3. Properties of selected formulations after 2 months of storage at  $25^\circ\text{C}$  and 50% RH.

Material	OTR.e	E	$\varepsilon$	Overall migration	
	$\text{cm}^3 \cdot \text{mm} \cdot \text{m}^{-2} \cdot \text{d}^{-1}$	MPa	%	$\text{mg} \cdot \text{dm}^{-2}$	
				In olive oil	In water
PLA-15 wt.-% G206/7	$25.0 \pm 3.0$	$673 \pm 29$	$226 \pm 69$	$4.6 \pm 2.4$	$0.2 \pm 0.2$
PLA-15 wt.-% G206/7-3 wt.-% C30B	$17.2 \pm 1.7$	$703 \pm 26$	$142 \pm 10$	$8.8 \pm 1.8$	$0.6 \pm 0.5$
PLA-20 wt.-% G206/7	$30.0 \pm 1.2$	$398 \pm 57$	$276 \pm 14$	$11.8 \pm 0.9$	$3.0 \pm 0.3$
PLA-20 wt.-% G206/7-3 wt.-% C30B	$20.7 \pm 0.1$	$503 \pm 32$	$167 \pm 16$	$17.6 \pm 1.5$	$3.9 \pm 0.3$

In the case of migration in the aqueous simulant, no significant differences were observed on the samples with or without C30B addition. Although this polyadipate is not soluble in water with a very low driving force, the eventual phase separation suffered during structural changes caused by annealing could increase the plasticizer exudation contributing to the overall migration observed in water.

## Conclusion

Novative nano-biocomposites based on plasticized PLA with the addition of O-MMT were elaborated by a melt intercalation method. The effect of the composition of these materials on the structure/properties relationships was analyzed. This study has shown that the addition of polyadipates could facilitate the process of clay intercalation and further exfoliation into the PLA matrix. This effect was particularly noticeable at high C30B concentrations, where the best dispersion of the nanofiller into the polymer matrix was observed.

At low O-MMT contents, silicate layers were easily dispersed into the PLA matrix and fairly good distribution was achieved. Oxygen barrier property showed a clear increase with C30B content, in the studied range. The best compromise between mechanical, thermal and barrier properties was achieved by the addition of 3 wt.-% C30B to PLA plasticized with polyadipates. Such formulations were stable after 2 months of storage at 25 °C and 50% RH. In addition to the reduction in OTR.e for around 30% compared to the unfilled plasticized matrix, such nano-biocomposites still showed  $\epsilon_B$  (%) values two orders of magnitude higher than that of the neat polymer.

The addition of filler to plasticized PLA matrices reduced the aging process when samples were stored at temperatures below their  $T_g$  values. However, when they were submitted to temperatures above their  $T_g$ s, O-MMT appeared to act as an effective nucleating agent to speed up PLA crystallization, which in turn favored the plasticizer exudation. This phenomenon promoted polyadipate migration, in particular into oil simulant.

Since the development of new biodegradable materials in food packaging applications requires further studies, some research work is currently ongoing to evaluate the effect of these novel nano-biocomposites on the final material properties, such as long term stability and biodegradability.

**Acknowledgements:** Authors would like to express their gratitude to *Condensia Química S.A* (Barcelona, Spain) for kindly supply of plasticizer. This work was partially financed by *Spanish Ministry of Science and Innovation* (project ref. MAT2008-06840-C02-01). Thanks are also extended to Dr. *Frederic Chivrac* and Dr. *Eric Pollet* (LIPHT-ECPM-Strasbourg) for their insight.

Received: October 30, 2009; Revised: February 4, 2010; Published online: May 17, 2010; DOI: 10.1002/mame.200900351

**Keywords:** aging; nanocomposites; organo-modified montmorillonite; polyadipate; poly(lactic acid)

- [1] E. Piorkowska, Z. Kulinski, A. Galeski, R. Masirek, *Polymer* **2006**, *47*, 7178.
- [2] H. Li, M. A. Huneault, *Polymer* **2007**, *48*, 6855.
- [3] O. Martin, L. Averous, *Polymer* **2001**, *42*, 6209.
- [4] N. Ljungberg, T. Andersson, B. Wesslén, *J. Appl. Polym. Sci.* **2002**, *86*, 1227.
- [5] N. Ljungberg, B. Wesslén, *J. Appl. Polym. Sci.* **2003**, *88*, 3239.
- [6] V. P. Martino, A. Jiménez, R. A. Ruseckaite, *J. Appl. Polym. Sci.* **2009**, *112*, 2010.
- [7] V. P. Martino, R. A. Ruseckaite, A. Jiménez, *Polym. Int.* **2009**, *58*, 437.
- [8] M. Zenkiewicz, J. Richert, *Polym. Test.* **2008**, *27*, 835.
- [9] M. D. Sanchez-Garcia, E. Gimenez, J. M. Lagaron, *Carbohydr. Polym.* **2008**, *71*, 235.
- [10] G. Choudalakis, A. Gotsis, *Eur. Polym. J.* **2009**, *45*, 967.
- [11] J. W. Rhim, S. I. Hong, C. S. Ha, *LWT-Food Sci. Technol.* **2009**, *42*, 612.
- [12] M. Alexandre, Ph. Dubois, *Mater. Sci. Eng.* **2000**, *28*, 1.
- [13] S. Sinha Ray, M. Okamoto, *Prog. Polym. Sci.* **2003**, *28*, 1539.
- [14] P. Bordes, E. Pollet, L. Averous, *Prog. Polym. Sci.* **2009**, *34*, 125.
- [15] Q. Zhou, M. Xanthos, *Polym. Degrad. Stab.* **2008**, *93*, 1450.
- [16] Q. Zhou, M. Xanthos, *Polym. Degrad. Stab.* **2008**, *94*, 327.
- [17] S. Sinha Ray, P. Maiti, M. Okamoto, K. Yamada, K. Ueda, *Macromolecules* **2002**, *35*, 3104.
- [18] J. H. Chang, Y. U. An, D. Cho, E. P. Giannelis, *Polymer* **2003**, *44*, 3715.
- [19] S. Bourbigot, G. Fontaine, S. Bellayer, R. Delobel, *Polym. Test.* **2008**, *27*, 2.
- [20] M. Pluta, M. A. Paul, M. Alexandre, Ph. Dubois, *J. Polym. Sci., Part B: Polym. Phys.* **2006**, *44*, 299.
- [21] C. Thellen, C. Orroth, D. Froio, D. Ziegler, J. Lucciarini, R. Farrell, N. A. D'Souza, J. A. Ratto, *Polymer* **2005**, *46*, 11716.
- [22] V. P. Martino, A. Jimenez, R. A. Ruseckaite, L. Averous, submitted to *Polym. Adv. Technol.* **2009**, manuscript ID: PAT-09-459.
- [23] M. Pluta, M. Muriaru, M. Alexandre, A. Galeski, Ph. Dubois, *Polym. Degrad. Stab.* **2008**, *93*, 925.
- [24] S. Solarski, M. Ferreira, E. Devaux, *Polym. Degrad. Stab.* **2008**, *93*, 707.
- [25] M. Pluta, M. A. Paul, M. Alexandre, Ph. Dubois, *J. Polym. Sci., Part B: Polym. Phys.* **2006**, *44*, 312.
- [26] UNE-EN 1186:2002 standard, AENOR 2002.
- [27] ASTM D882-01, *Standard Test Method for Tensile Properties of Thin Plastic Sheeting*, American Society for Testing and Materials 2001.
- [28] UNE-EN 1186-2:2002 standard, AENOR 2002.
- [29] UNE-EN 1186-3:2002 standard, AENOR 2002.
- [30] Commission Directive 2007/19/EC of 30 March 2007 amending Directive 2002/72/EC relating to plastic materials and articles intended to come into contact with food and Council Directive 85/572/EEC laying down the list of simulants to be used for testing migration of constituents of plastic materials and articles intended to come into contact with foodstuff.